

## Early Detection of Intravenous Infiltration Using Multi-frequency Bioelectrical Impedance Parameters: Pilot Study

Jae-Hyung Kim<sup>1</sup>, Beum-Joo Shin<sup>2</sup>, Seung-Wan Baik<sup>3</sup>, and Gye-Rok Jeon<sup>4\*</sup>

### Abstract

In this study, bioelectrical impedance analysis, which has been used to assess an alteration in intracellular fluid (ICF) of the body, was applied to detect intravenous infiltration. The experimental results are described as follows. Firstly, when infiltration occurred, the resistance gradually decreased with time and frequency i.e., the resistance decreased with increasing time, proportional to the amount of infiltrated intravenous (IV) solution. At each frequency, the resistance gradually decreased with time, indicating the IV solution (also blood) accumulated in the extracellular fluid (ECF) (including interstitial fluid). Secondly, the resistance ratio started to increase at infiltration, showing the highest value after 1.4 min of infiltration, and gradually decreased thereafter. Thirdly, the impedance ( $Z_C$ ) of cell membrane decreased significantly (especially at 50 kHz) during infiltration and gradually decreased thereafter. Fourthly, Cole-Cole plot indicated that the positions of ( $R$ ,  $X_C$ ) shifted toward left owing to infiltration, reflecting the IV solution accumulated in the ECF. The resistance ( $R_0$ ) at zero frequency decreased continuously over time, indicating that it is a vital impedance parameter capable of detecting early infiltration during IV infusion. Finally, the mechanism of the current flowing through the ECF, cell membrane, and ICF in the subcutaneous tissues was analyzed as a function of time before and after infiltration, using an equivalent circuit model of the human cell. In conclusion, it was confirmed that the infiltration could be detected early using these impedance parameters during the infusion of IV solution.

**Keywords:** Intravenous (IV) infiltration, Early detection, Impedance, Resistance, Impedance of cell membrane, Cole-Cole plot

### 1. INTRODUCTION

Insertion of an intravascular catheter is one of the most common invasive procedures in hospitals worldwide. Intravenous infusion and drug infusion into a blood vessel through a catheter are very common medical procedures for hospitalized patients. However, the failure rate of IV is estimated to be more than 20% [1]. Infiltration and extravasation are complications that can occur during the intravenous therapy administered via either peripheral or central venous access devices. Both can result in problems such as difficulty in siting of future venous access device, nerve

damage, infection, and tissue necrosis [2]. Infiltration occurs when intravenous (IV) fluid or medications leak into the surrounding tissue. Infiltration can be caused by improper placement or dislodgment of the catheter. Patient movement can cause the catheter to slip out or through the blood vessel lumen [3]. Extravasation is the leaking of vesicant drugs into the surrounding tissue. Extravasation can cause severe local tissue damage, possibly leading to delayed healing, infection, tissue necrosis, disfigurement, loss of function, and even amputation. In order to minimize the peripheral catheter-related complications, the insertion site should be inspected during each shift change and the catheter should be removed if signs of inflammation, infiltration, or blockage are present [4]. Infiltration events are graded from 1 to 4, with grade 4 events deemed the most severe [5]. Certain fluids and drugs can easily cause venous rupture when the venous endothelium and blood vessel walls are irritated, leading to IV infiltration or extravasation [6]. Recognizing the early signs and symptoms of infiltration can limit the amount of fluid that escapes into the tissue. Such signs and symptoms include local edema, skin blanching, skin coolness, leakage at the puncture site, pain, and feelings of tightness [7]. While immediate action using appropriate measures (i.e., dilution, extraction, antidotes, and supportive treatments) can decrease the need for surgical

<sup>1</sup>Research Institute of Nursing Science, Pusan National University, 49 Busandaehak-ro, Mulgeum-eup, Yangsan-si, Geongnam 50612, Korea

<sup>2</sup>Applied IT and Engineering, Pusan National University, 1268-50 Samryangjin-ro, Samyang, Jinyeong, Miryang, Gyeongnam 50463, Korea

<sup>3</sup>Dept. of Anesthesia and Pain Medicine, School of Medicine, Pusan National University, 20 Geumo-ro, Mulgeum-eup, Yangsan-si, Geongnam 50612, Korea

<sup>4</sup>Dept. of Biomedical Engineering, School of Medicine, Pusan National University, 20 Geumo-ro, Mulgeum-eup, Yangsan-si, Geongnam 50612, Korea

\*Corresponding author: grjeon@pusan.ac.kr

(Received: Jan. 19, 2017, Revised: Jan. 27, Accepted: Jan. 31, 2017)

This is an Open Access article distributed under the terms of the Creative Commons Attribution Non-Commercial License (<http://creativecommons.org/licenses/by-nc/3.0>) which permits unrestricted non-commercial use, distribution, and reproduction in any medium, provided the original work is properly cited.

intervention, many injuries may be prevented by following the established policy and procedures. However, timely surgical intervention, when necessary, can prevent more serious adverse outcomes [8]. As a result of the IV infiltration management program for pediatric patients undergoing peripheral IV infusion at a children's hospital, the IV infiltration was reduced to less than 1%. It was remarkably low compared with a comparison group who did not participate in the program, suggesting that the conducted program significantly reduced the occurrence of infiltration [9]. A safety event response team at Cincinnati Children's Hospital Center developed an improvement to reduce the peripheral intravenous (PIV) infiltration and extravasation. The improvement activities included development of a touch-look-compare method for hourly PIV site assessment, staff education and mandatory demonstration of PIV site assessment, and performance monitoring and sharing of compliance results [10]. In addition, the patented dual arms of the Venoscope® II contain two white and a red LEDs. This particular combination of lights, with different wavelengths, allowed the light to penetrate deeper into the subcutaneous tissue and to create the contrast necessary for the blood veins to stand out as dark lines within the illuminated orange tissue [11].

The research for detecting infiltration and extravasation during peripheral venous treatment has been performed using optical and electrical methods [12-14] because early detection of infiltration helps prevent the occurrence of serious injury that may require surgical corrections. An IV infiltration detection device coupled with fiber optics and an algorithm was proposed to detect the infiltration around the IV injection site noninvasively [12]. An early detection system (IV watch Model 400) of peripheral IV infiltration and extravasation events through continuous monitoring of the IV site using near-infrared (NIR) has been developed [13]. Researchers have also used ultrasound to examine the exogenous fluids injected into cutaneous and subcutaneous tissue. Ultrasound has been used to detect small volumes of fluids, such as cosmetic fillers and subcutaneous injections. These studies suggest that ultrasound may be a potential reference standard for the future evaluation of IV watch devices [14].

The early infiltration detection system is simple, reliable, economical, and should monitor the IV infiltration in a non-invasive manner for easy utilization in the nursing field. An infiltration detection system using bioelectrical impedance analysis (BIA) satisfies these conditions well because BIA is a safe, practical, and non-invasive method for measuring the components of biological tissues and materials [15]. BIA relies on the conduction of radio frequency electrical current by the fluid (water, interstitial fluid, and plasma), electrolytes, and permeability of the cell mem-

brane in the tissue [16]. BIA has been utilized to diagnose the diseases and to assess the hydration status, body composition, muscle-fat ratio, obesity degree, lean balance, edema, and nutritional status of the patients [17,18].

In this study, impedance was measured as a function of time during the IV infusion into the vein. In order to investigate any change in impedance caused by the infiltration, it was also measured as a function of time and frequency before and after the infiltration. The IV solution accumulated in the surrounding tissues during infiltration was evaluated using an equivalent circuit model of the human cell and the impedance parameters such as resistance, impedance of cell membrane, and the Cole-Cole diagram [19,20].

## 2. EXPERIMENTAL

### 2.1 Equivalent Circuit of Cell Membrane, ICF, and ECF

A basic understanding of normal body fluid physiology is required to be able to appreciate the nuances of fluid therapy. Total body water (TBW) accounts for approximately 60% of the total body weight. TBW is distributed between the intracellular fluid (ICF) compartment (approximately 66%) and the extracellular fluid (ECF) compartment (approximately 33%). These two spaces are separated by cell membranes. The ECF compartment is further subdivided into intravascular (8% TBW) and interstitial (25% TBW) spaces [21], and these compartments are separated by the capillary wall. The barriers (cell membranes) between the fluid compartments have different permeability to different solutes based on size, charge, and conformation. This selective permeability,

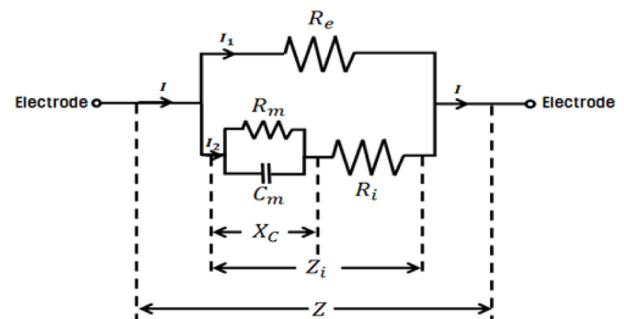


**Fig. 1.** The human body consists of resistance ( $R_e$ ,  $R_m$ ,  $R_i$ ) and capacitance ( $C_m$ ) connected in parallel or in series. In the parallel model, two or more resistors and capacitors are connected in parallel, with the current passing through the extracellular space at low frequencies and through the intracellular space at high frequencies.

**Table 1.** Description of symbols indicated in Fig. 1

Symbol	Description
$C_m$	Capacitance of cell membrane
$R_m$	Resistance of cell membrane
$R_e$	Resistance of ECF
$R_i$	Resistance of ICF
$X_C$	Reactance of cell membrane
$Z_i$	Impedance of $X_C$ and $R_i$
$Z$	Impedance of $Z_i$ and $R_e$
$I$	Current through both ECF and ICF
$I_1$	Current through only ECF
$I_2$	Current through both cell membrane and ECF

along with hydrostatic and oncotic forces (i.e., Starling forces), determines the movement of fluids and electrolytes between the compartments. Cells constituting human organs consist of ECF and ICF that behave as electrical conductors, whereas the cell membrane acts as an electrical resistance and capacitor [22,23].

Figure 1 indicates an equivalent circuit of a cell in the human body. Table 1 lists the descriptions of the indicated symbols in Fig. 1.

Since the resistance ( $R_m$ ) and the capacitance ( $C_m$ ) of the cell membrane are connected in parallel, the reactance ( $X_C$ ) of the cell membrane in Fig. 1 can be expressed as follows:

$$X_C = \frac{1}{\frac{1}{R_m} + j\omega C_m} = \frac{R_m}{1 + j\omega R_m C_m} = \frac{R_m}{1 + j2\pi f R_m C_m} \quad (1)$$

The reactance ( $X_C$ ) of the cell membrane and the resistance ( $R_i$ ) of the ICF connected in series can be expressed as

$$Z_i(j\omega) = R_i + X_C = R_i + \frac{1}{\frac{1}{R_m} + j\omega C_m} = R_i + \frac{R_m}{1 + j\omega C_m R_m} \quad (2)$$

The total impedance ( $Z$ ) of the cell model can be represented as

$$Z = \frac{1}{\frac{1}{R_e} + \frac{1}{Z_i}} = \frac{R_e Z_i}{R_e + Z_i} \quad (3)$$

The reactance ( $X_C$ ) of the cell membrane depends on the applied frequency. When the applied AC frequency is high,  $Z$  decreases, since  $X_C$  and  $Z_i$  decrease according to Eqs. (1) and (2). On the contrary, when the applied AC frequency is low,  $Z$  increases as the opposite phenomenon occurs.

Equation (2) can be separated into a real part and an imaginary part.

$$Z_i(j\omega) = R_i + \frac{\left(\frac{1}{R_m}\right)}{\left(\frac{1}{R_m}\right)^2 + \omega^2 C_m^2} - j \frac{\omega C_m}{\left(\frac{1}{R_m}\right)^2 + \omega^2 C_m^2} \quad (4)$$

When this equation is plotted in the Wessel diagram, the real values are on the x-axis, and the imaginary values are on the y-axis.

### 2.2 Cole-Cole plot

The flow of AC in the different compartments of the cellular spaces at different frequencies is usefully displayed as a Cole-Cole plot [24]. At very low frequencies ( $R_0$ ), the measurement is only resistive, and corresponds to the extracellular resistance. No current passes through the intracellular path because it cannot cross the capacitance ( $C_m$ ) of the cell membrane. As the applied AC frequency increases, the phase angle gradually increases as more AC is diverted away from ECF, and passes to ICF through the cell membrane with the capacitance. At high frequencies ( $R_\infty$ ), the capacitance of the cell membrane decreases sharply and can be neglected, hence AC enters the parallel resistances of the intracellular ( $R_i$ ) and extracellular compartments ( $R_e$ ). Thus, the reactance ( $X_C$ ) of the cell membrane is null; therefore, the entire impedance ( $Z$ ) is only resistive again and returns to the x-axis. Between  $R_0$  and  $R_\infty$ , AC passing through the capacitive path reaches a peak. The characteristic frequency ( $f_c$ ) is the frequency at which the current passing through the capacitive path reaches a peak, and is a useful measure of the properties of bioelectrical impedance.

To illustrate the Cole-Cole plot as shown in Fig. 2, Eq. (4) should be divided into the real part (on x-axis) and the imaginary part (on-y axis). X (real value) and Y (imaginary value) can be defined as follows.

$$X = R_i + \frac{\left(\frac{1}{R_m}\right)}{\left(\frac{1}{R_m}\right)^2 + \omega^2 C_m^2} \quad \text{and} \quad Y = \frac{\omega C_m}{\left(\frac{1}{R_m}\right)^2 + \omega^2 C_m^2} \quad (5)$$

These equations can be expressed in the form of a circle as follows:

$$\left(X - R_i - \frac{1}{2R_m}\right)^2 + Y^2 = \left(\frac{1}{2R_m}\right)^2 \quad (6)$$

$$\left(X - R - \frac{R_m}{2}\right)^2 + Y^2 = \left(\frac{R_m}{2}\right)^2 \quad (7)$$

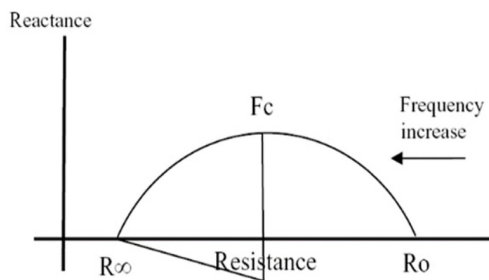


**Fig. 2.** Cole-Cole diagram: reactance vs. resistance in  $\beta$ -dispersion region.  $R_0$ : resistance at zero frequency (1 Hz),  $R_\infty$ : resistance at infinite frequency (100 MHz), and  $F_c$ : characteristic frequency.

Therefore, the resistance ( $R_m$ ) of the cell membrane and the resistance ( $R_i$ ) of ICF can be obtained by fitting the X values. The reactance ( $X_C$ ) and the capacitance ( $C_m$ ) of the cell membrane can be obtained by fitting the Y values.

### 2.3 Subjects

In this study, two healthy adults were selected as experimental subjects to conduct a small-scale exploratory clinical trial led by researchers. Prior to participation in this study, the purpose of this study was explained to the subjects and their written consents were obtained. The subjects were 2 males with a mean ( $\pm$ SD) age of  $61.0 \pm 2.0$  years, mean height of  $168.0 \pm 3.0$  cm, mean weight of  $68.0 \text{ kg} \pm 3.0 \text{ kg}$ , and mean body mass index (BMI) of  $24.23 \pm 0.34 \text{ kg/m}^2$ . All subjects were free of any known chronic illnesses. This study was approved by the IRB committee of Pusan National University Yangsan Hospital (IRB No. 03-2016-017).

### 2.4 Peripheral intravenous injection and induced infiltration

Electrodes (separated by 12 cm) intended for applying the current and collecting the voltage were attached to both sides of the transparent dressing at the infusion site. Ag/AgCl medical electrodes (2223H, 3M, Korea) with foam tape and sticky gel) were used to minimize error between electrode and the skin. After inserting the PIV (peripheral intravenous) catheter into a vein of the inner forearm of the subjects, the infiltration was deliberately induced by pushing the needle through the vein wall into the subcutaneous tissue. Subsequently, a transparent dressing (10.2 cm  $\times$  7.4 cm, Sewoon Ltd., Korea) was immediately placed at the infusion site to observe the swelling of the tissue around the infiltrated vein visually. Bioimpedance was measured as a function of time and frequency before and after infiltration, using bioelectrical

impedance spectroscopy (called Vector) developed by Kim [25]. AC with 8 different frequencies (20, 50, 100, 200, 300, 500, 700, and 1000 kHz) was applied to the electrodes to measure BI.

## 3. RESULTS AND DISCUSSIONS

### 3.1 Resistance as a function of time before and after infiltration

The resistance of the body to the flow of alternating current is related to the volume (or amount) of fluid in the body [26]. An acute (minor) change in the fluid status can alter the resistance of the human body [27,28]. According to experiments performed with IV infusion [29], the bioimpedance analysis is sufficiently sensitive to detect minute changes in the volume of fluid in the body.

Figure 3 shows the change in resistance as a function of time during the IV infusion into the vein. BI (before infiltration) indicates the instance when the IV solution is properly infused into the vein. AI (at infiltration) indicates the instance when the infiltration occurs. The resistance decreased with increasing frequency. At each frequency, the resistance gradually decreased over time, proportional to the amount (60 ggt./min.) of IV solution leaking from the vein owing to infiltration, indicating the IV solution (and blood products) accumulated in the ECF (including interstitial fluid). Scheltinga et al. applied an alternating current with 800  $\mu$ A and 50 kHz to the arm of the subject while injecting a saline

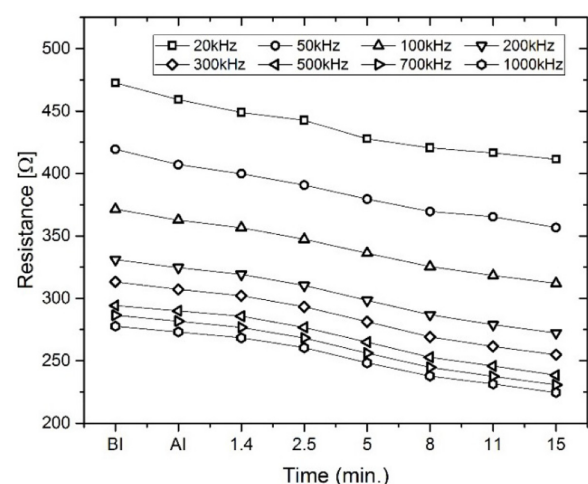


**Fig. 3.** Resistance as a function of time. As the IV solution continues to leak from the vein, resistance decreases gradually over time. BI (before infiltration) indicates the instance when the IV solution is properly infused into the vein. AI (at infiltration) indicates the instance when the infiltration occurs.

infusion into the subject for 15 min. They reported a decrease in the resistance from 5 min after the IV infusion [28]. In this experiment, an intentional infiltration was induced during the IV infusion, and the resistance was measured at a narrow IV site using multi-frequency impedance spectroscopy. The resistance gradually decreased over time, which indicates that the accumulation of the IV solution from the vein gradually increased in the subcutaneous tissue. Therefore, when the IV solution is infused, it is suspected that the infiltration occurs if the resistance continues to decrease.

**3.2 Resistance ratio as a function of time before and after infiltration**

Bioimpedance spectroscopy can accurately measure the resistance of body fluid compartments (ECF, ICF). The resistance ratio of ICF to ECF should reflect the relative volume of these compartments. As dialysis patients accumulate excess fluid in their extracellular compartment, this ratio may prove useful in the evaluation of dry weight [30]. Applying the resistance ratio to the infiltration phenomenon can lead to the following concept if infiltration occurs during the IV infusion into the vein, the resistance ratio will vary with time and frequency because the IV solution accumulates in the ECF.

Figure 4 shows the resistance ratio at 200, 300, 500, 700, and 1000 kHz to that at 20 kHz. At 20 kHz, the current flows only to the ECF because it cannot pass through the cell membrane. Hence, the resistance measured is high. On the other hand, AC with a frequency of 50 kHz or more can pass through the cell

membrane. As the frequency of the applied current increases, the current flowing to the ICF increases and the resistance decreases further. Therefore, the resistance ratio with respect to frequency can reflect this change in resistance. The resistance ratios start increasing at AI, showing the highest value at 1.4 min after the infiltration, and gradually decrease thereafter. Thus, the infiltration during IV infusion can be detected using the resistance ratio.

**3.3 Resistance as a function of frequency before and after infiltration**

Whether a cell membrane behaves as a resistor or capacitor depends on the frequency of the applied current. When an alternating current with a frequency lower than 50 kHz ( $2.1 \times 10^{-11} eV$ ) was applied to the IV site, the resistance was measured to be relatively high because the current only flowed into the narrow ECF, which is composed of adipose tissue. Only a small amount of current finds “the path of least resistance” through a capillary [31]. Hence, the decreasing resistance over time at 20 kHz ( $8.4 \times 10^{-11} eV$ ) reflects the IV solution accumulating in the ECF after infiltration. On the other hand, when an alternating current with a frequency higher than 50 kHz is applied to the IV site, the current has sufficient energy to pass through the cell membrane; therefore, the current flows into the ICF with a larger internal cross-sectional area. Thus, the current flows through both ECF and ICF. As the frequency increases, more current flows into ICF, which further reduces the resistance.

Figure 5 shows the resistance as a function of frequency before and after the infiltration. The resistance decreased exponentially

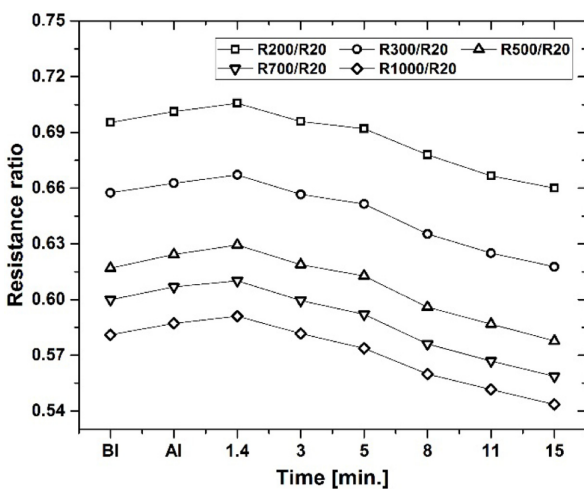


**Fig. 4.** Resistance ratio as a function of time before and after infiltration. The resistance ratios start increasing at AI, showing the highest value at 1.4 min after the infiltration, and gradually decrease thereafter.

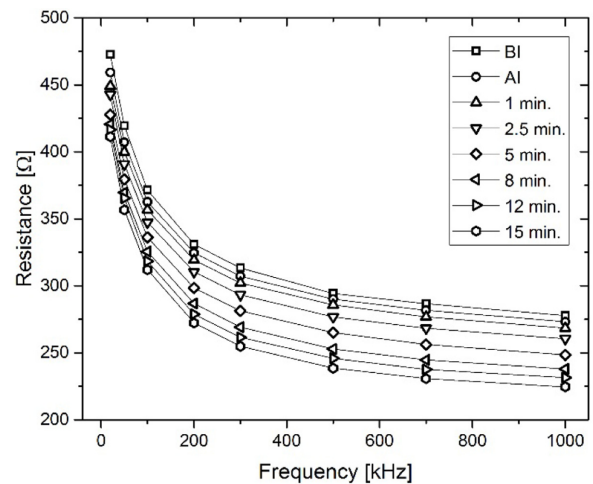


**Fig. 5.** Resistance as a function of frequency. The resistance decreased exponentially with respect to frequency. At each frequency, the decrease in resistance was almost constantly reduced over time.

with respect to frequency. At each frequency, the decrease in resistance was almost constantly reduced over time. However, the decrease in resistance owing to the infiltration was clearly observed in the frequency range of 20 - 100 kHz. It is believed that the IV solution and blood components leak from the vein during infiltration and accumulate in the ECF. This can be a useful parameter for the early detection of infiltration.

### 3.4 Impedance of cell membrane as a function of time before and after infiltration

The impedance ( $Z_C$ ) of cell membrane is a measure of the function of the cell membrane [31]. The cell membrane can store charge for a short period of time and slow down the current flow. The cell membrane acts as a resistor when the frequency of the applied current is low and as an accumulator when the frequency of the applied current is high. At a low frequency below 50 kHz, the current cannot flow through the cell membrane. At these frequencies, the cell membranes act as resistors because current cannot pass through the cell membranes. Therefore, at low frequencies, any current conducting through the body only passes through ECF. On the other hand, currents with frequencies higher than 50 kHz can pass through the cell membranes and flow through the ICF as well as ECF.

Figure 6 shows the impedance ( $Z_C$ ) of cell membrane as a function of time during the IV infusion into the vein. When infiltration occurred during the IV infusion,  $Z_C$  decreased significantly at AI and subsequently decreased. As the frequency of the applied AC increased, the ability of the cell membrane to slow down the flowing current was significantly reduced, and

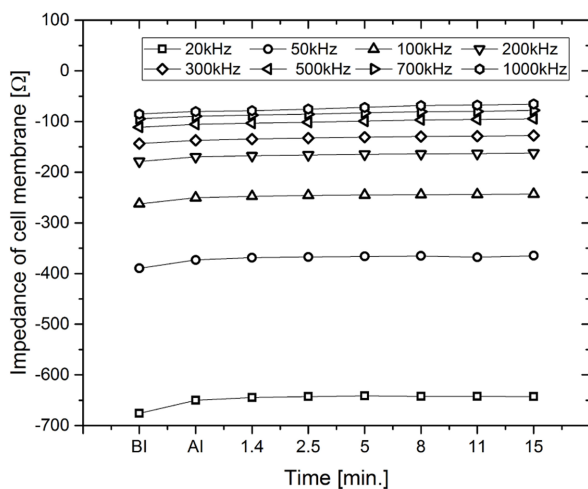


**Fig. 6.** Impedance ( $Z_C$ ) of cell membrane as a function of time. When infiltration occurred during the IV infusion,  $Z_C$  decreased significantly at AI and subsequently decreased.

hence,  $Z_C$  decreased. The impedance of cell membrane was most evidently reduced at 20 kHz during the infiltration. It is concluded that  $Z_C$  was reduced because IV solution adsorbs to the cell membrane due to the infiltration and weakened the ability of the cell membrane to slow down the current.

### 3.5 Cole-Cole Plot: reactance versus resistance

The impedance spectra of the electric circuit can be obtained using bioelectrical impedance spectroscopy (BIS). The curve obtained by these values is called a Cole-Cole plot (or impedance locus), and the shape of the curve depends on the characteristics of the circuit [32,33]. The equivalent circuit of a human cell consists of the ECF and ICF resistances and the cell membrane capacitance. The computer extrapolates the admittance locus represented by the equation of the derived Cole and Cole distribution circuit in the frequency range of 1 kHz to 500 kHz. From this equation, it is possible to extract the extracellular fluid resistance ( $E_{ECF}$ ), intracellular fluid resistance ( $R_{ICF}$ ), membrane capacitance ( $C_m$ ), and time constant ( $T_0$ ) of structural relaxation ( $\beta$  dispersion). Variations of the tissue impedance, when measured as a function of frequency, result from changes in the structural properties of the tissue; these measurements provide valuable information about the volume and distribution of both ICF and ECF. When a low-frequency voltage is applied to the tissue, the current mainly flows through the ECF, whereas at high frequencies it flows through both ECF and ICF.

Figure 7 shows the reactance versus resistance (i.e., the Cole-Cole plot) for different frequencies. The symbols at the bottom right are values measured at 20 kHz and the frequency increases in the counterclockwise direction. At zero (or low) frequency, the current cannot penetrate the cell membrane, which acts as an insulator; therefore, the current passes through the ECF, which is responsible for the measured  $R_0$  of the body. At finite frequency (or a very high frequency), the cell membrane behaves as a perfect (or near perfect) capacitor; therefore, the total body water reflects the combined  $R$  of both ICF and ECF. At a lower frequency (20 and 50 kHz), the measured values moved in the upper left direction owing to infiltration. At each frequency, the measured values of ( $R$ ,  $X_C$ ) shifted toward left owing to infiltration, reflecting the IV solution being accumulated in the ECF. These phenomena have been observed in impedance studies conducted by other researchers as well. Nescolarde et al. investigated the impedance at 50 kHz in a calf muscle before and after an injury of soccer players, and reported that the resistance of the more severely injured muscle was further decreased (11.9% in grade 1, 20.6% in



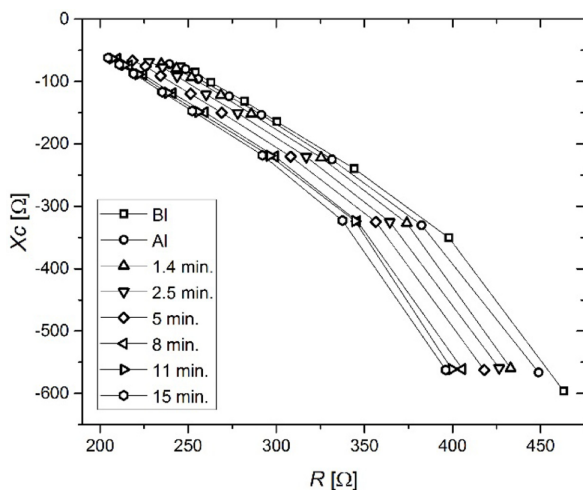


**Fig. 7.** Cole-Cole plot; its relationship with resistance ( $R$ ), reactance ( $X_C$ ), and the frequency of the applied current. At each frequency, the measured values of ( $R$ ,  $X_C$ ) shifted toward left owing to infiltration, reflecting the IV solution being accumulated in the ECF.

grade 2, and 23.1% grade 3) compared to the non-injured muscle ( $68 \Omega$ ). Their findings indicated that the decreases in  $R$  reflected a localized accumulation of fluid [34].

Figure 8 shows the resistance at zero frequency as a function of time. These values are obtained by extrapolating the curves in the direction (clockwise) of zero frequency in the Cole-Cole plot shown in Fig. 8. When infiltration occurs during the IV infusion, the resistance ( $R_c$ ) decreases because the IV solution accumulates in the ECF (mainly interstitial fluid). Since the resistance ( $R_0$ ) at zero frequency reflects the current flowing through the ECF, the steady decrease in resistance over time can be attributed to the

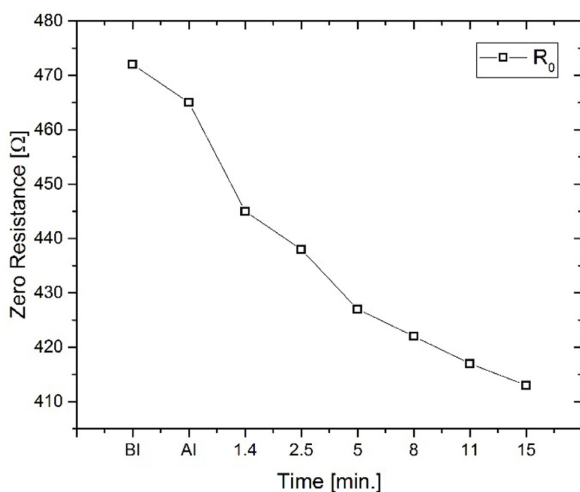


**Fig. 8.** Zero resistance ( $R_0$ ) as a function of time before and after infiltration. The resistance at zero frequency decreases continuously over time, indicating that it is an important impedance parameter that can detect infiltration.

infiltration. The resistance at zero frequency decreases continuously over time, indicating that it is an important impedance parameter that can detect infiltration.

### 3.6 Discussions

Infiltration is a condition wherein an infused IV solution inadvertently leaks into the soft subcutaneous tissue surrounding a hypodermic needle site. The current methods of detection of infiltration by medical staff are fairly subjective and are potentially prone to error [35].

So far, the infiltration detection systems have been developed using visible light and near-infrared LEDs as light sources. In such systems, a significant decrease in the reflection of light from the skin above the IV site was recognized as infiltration compared to the reflection of light before infiltration. However, the occurrence of infiltration was recognized through a reduction of the reflected light from the skin surface, and the IV solution penetrating into the subcutaneous tissue could not be detected by such a method.

In this study, infiltration was deliberately induced by puncturing the vein wall of the subjects with an injection needle during the IV infusion. Various data about the IV solution leaking from the vein into the subcutaneous tissue was acquired using the impedance parameters (resistance, reactance) and the Cole-Cole plot. When the infiltration occurred, the resistance gradually decreased at 8 frequencies ranging from 20 to 1000 kHz. The resistance ratio was used to determine the infiltration. The resistance ratio starts increasing at infiltration, showing the highest value at 1.4 min after infiltration, and decreased gradually thereafter. The Cole-Cole plot indicated that at lower frequencies (20 and 50 kHz), the movement of the measured values owing to infiltration was well visible in the upper left direction. The positions of ( $R$ ,  $X_C$ ) shifted to the left owing to infiltration, reflecting the IV solution being accumulated in the ECF. These phenomena have been observed in impedance studies conducted by other researchers as well. Nescolarde et al. measured the reactance versus resistance at 50 kHz in a calf muscle before and after injuries of football players, and reported that the resistance for a more severely injured muscle was further reduced (11.9% in grade 1, 20.6% in grade 2, and 23.1% grade 3) compared to the non-injured muscle ( $68 \Omega$ ).

## 4. CONCLUSIONS

In this study, bioelectrical impedance analysis, which has been used to assess an alteration in the ICF of the body, was introduced

for early detection of infiltration. The bioelectrical impedance (resistance and reactance) was measured as a function of time and frequency using bioelectrical impedance spectroscopy. When the infiltration occurred, the resistance gradually decreased over time, proportional to the amount of IV solution leaking from the vein owing to infiltration. Using an equivalent circuit model and the resistance at 20 kHz, the IV solution leaking from the vein was confirmed to be accumulated in the ECF. In addition, when a current with a frequency higher than 50 kHz ( $2.1 \times 10^{-10} eV$ ) was applied to the IV site, the resistance further decreased, because the applied AC was sufficiently strong to penetrate the cell membrane and flowed into the ICF as well as ECF.

The result of applying the impedance parameters such as resistance, resistance ratio, impedance of cell membrane, and Cole-Cole plot to the infiltration can be summarized as follows. Firstly, the resistance decreased with increasing time (proportional to the amount of infiltrated IV solution). At each frequency, the resistance gradually decreased with time, indicating the fluid (and blood) accumulated in the ECF and ISF. Secondly, the resistance ratio started to increase at infiltration, showing the highest value after 1.4 min of infiltration, and gradually decreased thereafter. Thirdly, when the infiltration occurs during the IV infusion into the vein, the impedance of cell membrane decreased significantly (especially at 50 kHz) during infiltration and gradually decreased thereafter. Finally, the Cole-Cole plot indicated that the positions of ( $R_c, X_c$ ) shifted to the left owing to infiltration, reflecting the IV solution being accumulated in the ECF. The resistance ( $R_0$ ) at zero frequency decreased continuously over time, indicating that it is an important impedance parameter capable of detecting early infiltration during the IV infusion.

In the future, clinical applications of BIS (Bioelectrical impedance spectroscopy) based IV infiltration will be performed on the rehabilitation patients in rehabilitation hospitals and cancer patients in oncology.

## ACKNOWLEDGMENT

This research was supported by Basic Science Research Program through the National Research Foundation of Korea (NRF) funded by the Ministry of Science, ICT and Future Planning (2015R1A2A2A04003415).

## REFERENCES

- [1] Startup launches device for early detection of IV tissue infiltration to reduce complications (2016). <http://www.fiercebiotech.com/medical-devices/startup-launches-device-for-early-detection-iv-tissue-infiltration-to-reduce> (accessed on Jan., 3, 2017).
- [2] L. Dougherty, "IV therapy: recognizing the differences between infiltration and extravasation," *British Journal of Nursing*, Vol. 17, No. 14, pp. 896-901, 2008.
- [3] Complications of Peripheral I.V. Therapy, Lippincott Nursing Center (2015). [http://www.nursingcenter.com/ncblog/february-2015-\(1\)/complications-of-peripheral-i-v-therapy](http://www.nursingcenter.com/ncblog/february-2015-(1)/complications-of-peripheral-i-v-therapy) (accessed on Jan., 4, 2017).
- [4] J. L. Thigpen, "Peripheral intravenous extravasation: nursing procedure for initial treatment," *Neonatal Network*, Vol. 26, No. 6, pp. 379-384, 2007.
- [5] L. Hadaway, "Infiltration and extravasation," *American Journal of Nursery*, Vol. 107, No. 8, pp. 64-72, 2007.
- [6] S. M. Park, I. S. Jeong, S. S. Jun, "Identification of risk factors for intravenous infiltration among hospitalized children: a retrospective study," *PLOS ONE*, 1-8, Jun 28, 2016.
- [7] L. Hadaway, "Protect patients from I.V. infiltration," *American Nurse Today*, Vol. 5, No. 2, 2010. <https://www.americannursetoday.com/protect-patients-from-i-v-infiltration-3/> (accessed on Jan., 5, 2017)
- [8] D. Doellman, L. Hadaway, L. A. Bowe-Geddes, M. Franklin, J. LeDonneJ, L. Papke, et al., "Infiltration and extravasation: update on prevention and management," *Journal of Infusion Nursing*, Vol. 32, No. 4, pp. 203-211, 2009.
- [9] S. M. Park, I. S. Jeong, K. L. Kim, K. J. Park, M. J. Jung, S. S. Jun, "The effect of intravenous infiltration management program for hospitalized children," *Journal of Pediatric Nursing*, Vol. 31, pp. 172-178, 2016.
- [10] B. F. Tofani, S. A. Rineair, C. H. Gosdin, P. M. Pilcher, S. McGee, K. R. Varadarajan, et al., "Quality improvement project to reduce infiltration and extravasation events in a pediatric hospital," *Journal of Pediatric Nursing*, Vol. 27, No. 6, pp. 682-689, 2012.
- [11] Emergency Care (2015). <http://www.venoscope.com/iv-vein-finder/> (accessed on Sept. 13, 2016).
- [12] Wintec, LLC, Optical detection of intravenous infiltration, US 7,826,890 B1, USA, 2005.
- [13] An optical device for detecting intravenous infiltration (2006). <http://www.ivteam.com/optical-iv.pdf> (accessed on Dec., 21, 2016).
- [14] Ultrasound Detection of Peripheral IV Infiltration (2013), <https://clinicaltrials.gov/ct2/show/NCT01800552> (accessed on Jan., 6, 2017).
- [15] U. G. Kyle, I. Bosaeus, A. D. De Lorenzo, P. Deurenberg, M. Elia, J. M. Gómez, et al., "Bioelectrical impedance analysis-part 1: review of principles and methods," *Clinical Nutrition*, Vol. 23, No. 5, pp. 1226-1243, 2004.
- [16] L. C. Ward, "Segmental bioelectrical impedance analysis: an update," *American Journal of Clinical Nutrition*, Vol. 15, No. 5, pp. 424-429, 2012.
- [17] S. Berlit, J. Brade, B. Tuschy, E. Földi, U. Walz-Eschenlohr, H. Leweling, et al., "Whole-body versus segmental bioelectrical impedance analysis in patients with edema of the upper limb after breast cancer treatment," *Anticancer*



- Research*, Vol. 33, No. 8, pp. 3403-3406, 2013.
- [18] R. Buffa, E. Mereu, O. Comandini, M. E. Ibanez, E. Marini, "Bioelectrical impedance vector analysis (BIVA) for the assessment of two-compartment body composition," *European Journal Clinical Nutrition*, Vol. 68, No. 11, pp. 1234-1240, 2014.
- [19] S. F. Khali, M. S. Mohktar, F. Ibrahim, "The theory and fundamentals of bioimpedance analysis in clinical status monitoring and diagnosis of diseases," *Sensors*, Vol. 14, pp. 10895-10928, 2014.
- [20] I. S. Grimnes, O. G. Martinsen, *Bioimpedance and Bioelectricity Basics*, Academic Press, London, 2015.
- [21] E. Mazzaferro, L. L. Powell, "Fluid therapy for the emergent small animal patient: crystalloids, colloids, and albumin products," *Veterinary Clinics of North America: Small Animal Practice*, Vol. 43, No. 4, pp. 721-734, 2013.
- [22] J. H. Kim, S. S. Kim, S. H. Kim, S. W. Baik, G. R. Jeon, "Bioelectrical impedance analysis at popliteal regions of human body using BIMS," *Journal of Sensor Science & Technology*, Vol. 25, No. 1, pp.1-7, 2016.
- [23] E. Hernández-Balaguera, E. López-Doladob, J. L. Polo, "Obtaining electrical equivalent circuits of biological tissues using the current interruption method, circuit theory and fractional calculus," *Royal Society of Chemistry*, Vol. 6, pp. 22312-22319, 2016.
- [24] S. Kumar, A. Dutt, S. Hemraj, S. Bhat, B. Manipadybhima, "Phase angle measurement in healthy human subjects through bio-impedance analysis," *Iranian Journal of Basic Medical Sciences*, Vol. 15, No. 6, pp. 1180-1184, 2012.
- [25] B. C. Kim, C. M. Kim, C. H. Lee, Multi-channel impedance measuring method and multi-channel impedance measuring instrument, WO 2014/035040 A1, Patent PCT/KR2013/005779.
- [26] E. C. Hoffer, C. K. Meador, D. C. Simpsons, "Correlation of whole-body impedance with total body water volume," *Journal of Applied Physiology*, Vol. 27, pp. 531-534, 1969.
- [27] A. Barnett, "Electrical method for studying water metabolism and translocation in body segments," *Experimental Biology and Medicine*, Vol. 44, pp. 142-147, 1940.
- [28] B. T. Tender, "Automatic reading of biological impedance," *Journal of Medical Engineering & Technology*, Vol. 2, Issue 2, pp. 70-73, 1978.
- [29] M. R. Scheltinga, D. O. Jacobs, T. D. Kimbrough, D. W. Wilmore, "Alterations in body fluid content can be detected by bioelectrical impedance analysis," *Journal of Surgical Research*, Vol. 50, pp. 461-468, 1991.
- [30] D. M. Spiegel, K. Baashir, and B. Fisch, "Bioimpedance resistance ratios for the evaluation of dry weight in hemodialysis," *Clinical Nephrology*, Vol. 53, No. 2, pp. 108-114, 2000.
- [31] Bioelectrical impedance analysis (2015), <http://nutrition.uvm.edu/bodycomp/bia/bia-toc.html> (accessed on Dec., 12, 2016).
- [32] K. S. Cole, R. H. Cole, "Dispersion and adsorption in dielectrics," *Journal of Chemical Reviews*, Vol. 9, pp. 341-352, 1941.
- [33] H. Kanni, M. Haeno, K. Sakamoto, "Electrical measurement of fluid distribution in legs and arms," *Medical Progress through Technology*, Vol. 12, pp. 159-170, 1987.
- [34] Nescolarde, J. Yanguas, H. Lukaski, X. Alomar, J. Rosell-Ferrer, G. Rodas, "Localized bioimpedance to assess muscle injury," *Physiology Measurement*, Vol. 34, pp. 237-245, 2013.
- [35] J. A. Jambulingam, R. McCrory, L. West, O. T. Inan, "Non-invasive, multi-modal sensing of skin stretch and bioimpedance for detecting infiltration during intravenous therapy," *38th Annual International Conference of the IEEE Engineering in Medicine and Biology Society* (2016), 16-20, 2016.